

1n- and 2n- transfer with the Borromean nucleus ${}^6\text{He}$ near the Coulomb barrier

A. Chatterjee,^{1,2} A. Navin,^{1,*} A. Shrivastava,² S. Bhattacharyya,¹ M. Rejmund,¹ N. Keeley,^{3,4} V. Nanal,⁵ J. Nyberg,⁶ R.G. Pillay,⁵ K. Ramachandran,² I. Stefan,¹ D. Bazin,⁷ D. Beaumel,⁸ Y. Blumenfeld,⁸ G. de France,¹ D. Gupta,⁸ M. Labiche,⁹ A. Lemasson,¹ R. Lemmon,⁹ R. Raabe,¹ J.A. Scarpaci,⁸ C. Simenel,³ and C. Timis¹⁰

¹*GANIL, CEA/DSM - CNRS/IN2P3, Bd Henri Becquerel,
BP 55027, F-14076 Caen Cedex 5, France*

²*Nuclear Physics Division, Bhabha Atomic Research Centre, Mumbai 400085, India*

³*DSM/IRFU/SPhN, CEA Saclay, F-91191 Gif sur Yvette, France*

⁴*Department of Nuclear Reactions, The Andrzej Soltan Institute for Nuclear Studies,
Hoza 69, PL-00-681 Warsaw, Poland*

⁵*DNAP, Tata Institute of Fundamental research, Mumbai 400005, India*

⁶*Department of Physics and Astronomy,
Uppsala University, Uppsala, Sweden*

⁷*National Superconducting Cyclotron Laboratory,*

Michigan State University, East Lansing, Michigan, 48824, USA

⁸*Institut de Physique Nucléaire, IN2P3-CNRS, 91406 Orsay, France*

⁹*CRLC, Daresbury Laboratory, Daresbury, Warrington, WA4 4AD, U.K.*

¹⁰*Department of Physics, University of Surrey, Guildford, GU2 7XH, U.K.*

Abstract

Angular distributions for 1n and 2n transfer are reported for the ${}^6\text{He} + {}^{65}\text{Cu}$ system at $E_{lab} = 22.6$ MeV. For the first time, triple coincidences between α particles, neutrons and characteristic γ -rays from the target-like residues were used to separate the contributions arising from 1n and 2n transfer. The measured differential cross-sections for these channels, elastic scattering and fusion have been analyzed using a Coupled Reaction Channels approach. The measured large ratio of the 2n/1n cross section and the strong influence of 2n transfer on other channels point towards the dominance of a di-neutron configuration of ${}^6\text{He}$ in the reaction mechanism.

PACS numbers: 25.60.-t, 24.50.+g, 25.70.Jj

Reactions near the Coulomb barrier have been shown to be an ideal tool to study the effect of multidimensional tunneling and obtain information about the structure of the interacting nuclei [1]. New features arising from the weak binding in nuclei far from stability on reactions near the Coulomb barrier have been recently discussed [2]. Neutron rich nuclei near the drip line, especially Borromean nuclei offer a unique environment to study neutron correlations at low densities, which are necessary inputs for nuclear structure models and the study of neutron stars. Theoretical analyses suggest that at low neutron density, strong spatial di-neutron correlations are expected [3, 4]. Such correlations have been theoretically studied in two-neutron Borromean nuclei like ${}^6\text{He}$ and ${}^{11}\text{Li}$ [5]. The structure of the lightest two-neutron halo nucleus, ${}^6\text{He}$, with an inert α core and known α -n interaction has been investigated via a variety of techniques [6–9], mainly at energies well above the Coulomb barrier.

The ratio of the $2n/1n$ transfer cross section can provide information about the structural correlation of neutrons in ${}^6\text{He}$. The cigar shape, where the two neutrons are expected to lie on opposite sides of the α particle, should preferentially populate ${}^5\text{He}$ by $1n$ transfer while the di-neutron configuration should be responsible mainly for $2n$ transfer [10]. The recently reported charge radii of ${}^{6,8}\text{He}$ provide an independent method of studying correlations in these Borromean nuclei [11]. Michel *et al.* have investigated the Wigner threshold law in weakly-bound nuclei using the Gamow shell model [12]. The authors show the influence of the Wigner cusp on the spectroscopic factors. Thus, the study of transfer angular distributions with Borromean nuclei is of interest in the context of this general phenomenon observed in various fields of physics [13].

Alpha-n coincidences measured in the ${}^6\text{He} + {}^{209}\text{Bi}$ system, at a lab energy of 22 MeV, showed the relative dominance of the $2n$ channel [14, 15]. Reactions on medium-mass targets are experimentally more challenging and are also controversial with respect to the influence of weak binding on the fusion process [16]. Theoretical treatment of reactions involving Borromean projectiles, especially at energies near the barrier, represents a complex problem as calculations have to include the unbound spectrum of a four-body system. However, state-of-the-art continuum discretized coupled-channel calculations that take into account the three-body nature of ${}^6\text{He}$ [17, 18] or its simplification as a $2n+\alpha$ cluster [19] have been performed. These calculations can presently compute only elastic scattering and breakup reactions. A theoretical formalism that can simultaneously describe elastic scattering, transfer and breakup reactions is desirable but not yet available.

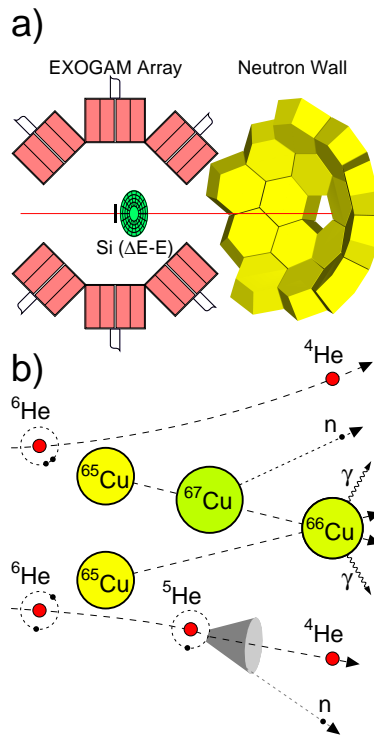


FIG. 1: (color online) Schematic of (a) The experimental setup. (b) Reaction mechanism for 2n- and 1n- transfer

With the motivation of understanding the Borromean structure and its influence on reactions around the Coulomb barrier, the present work reports a novel triple coincidence measurement of angular distributions of transfer channels with ISOL beams. A first theoretical attempt, for Borromean nuclei, towards understanding the importance of the role of coupling transfer channels to elastic scattering and fusion is also presented.

Intense radioactive ion beams ($\sim 4 \times 10^7$ pps) of ${}^6\text{He}$ at an energy of 22.6 MeV were obtained from the ISOL facility SPIRAL at GANIL. The target was a 2.6 mg/cm² thick self supporting foil of ${}^{65}\text{Cu}$, isotopically enriched to 99.7 %. Beam intensities were measured with a high stability current amplifier connected to a Faraday cup. The experimental setup (Fig. 1a) consisted of an annular Si telescope, the EXOGAM γ array [20] with 11 Compton suppressed clovers, and a neutron array consisting of 45 liquid scintillator elements [21].

Charged particles were detected and identified in an annular Si telescope consisting of ΔE ($\sim 50\mu$) and E ($\sim 500\mu$) elements with active inner and outer diameters of 22 mm and 70 mm covering an angular range of $\sim 25^\circ$ to 60° at a distance of 2.5 cm from the target. The angular resolution was $\simeq 1.7^\circ$. The solid angles of each ring/sector combination of

the annular telescope were determined both from simulations and comparison with elastic scattering measurements on a Au target. The energy resolution for elastically scattered particles was $\simeq 300$ keV. The Neutron Wall consisted of 45 hexagonal detectors, located at a distance of 55 cm from the target and covered $\simeq 18\%$ of 4π [21]. The time of flight (TOF) was obtained with respect to the E detector of the annular telescope. The TOF resolution was $\simeq 3$ ns (corresponding to an energy resolution of 270 keV at $E_n=1.5$ MeV). Neutrons were separated from γ -rays by two-dimensional gates in the plot of TOF vs. pulse-shape discrimination and detected at mean angles of 19° , 30° , 35° , 47° , and 57° with an angular resolution of $\pm 6.5^\circ$. Small corrections for cross talk between the neutron detectors were suitably taken into account [22]. The absolute efficiencies of the neutron detectors, as a function of energy, were determined from a comparison of the measured neutron spectra from a ^{252}Cf source placed at the target position and the known multiplicity and spectral shape [23]. The measured efficiencies compared well with Monte Carlo simulations of the neutron array [22]. Eleven Compton suppressed clover detectors located at a distance of 14.7 cm from the target were used to select the residual nuclei from the measurement of their characteristic γ -rays. The cross sections for various evaporation residue channels were obtained from the yields of characteristic γ -rays, following the method outlined in Ref. [16]. The sum of the measured evaporation residue cross sections was used to obtain the total fusion cross section. Statistical model calculations using the code CASCADE [24] were made and showed good agreement for all the residues except ^{66}Cu . The yield of ^{66}Cu from fusion evaporation is negligible ($\approx 5\%$); it is produced mainly by 1n and 2n transfer (see also [16]).

Fig. 1b shows a schematic of the reaction mechanism indicating that the final state, as a result of the Borromean nature of ^6He , is similar in both 1n and 2n neutron transfer. In both cases we have a neutron, an α particle and γ -rays from the excited ^{66}Cu residue. The figure also shows that there is an angular correlation between α particles and neutrons for 1n-transfer but not for 2n-transfer. Triple coincidences between n , α and γ -rays from the excited ^{66}Cu residue were used to deconvolute the 1n and 2n transfer contributions and also to eliminate projectile breakup. The extraction of the transfer cross section was made as follows. Data with conditions for neutron, α particle and γ transitions in ^{66}Cu were first selected. These events were then used to obtain the angles and energies for the selected neutrons and α particles and their relative angles $\theta_{n\alpha}$ and energies $E_{n\alpha}$. The population of the $3/2^-$ ground state of ^5He was verified from the measured correlation between the $\theta_{n\alpha}$

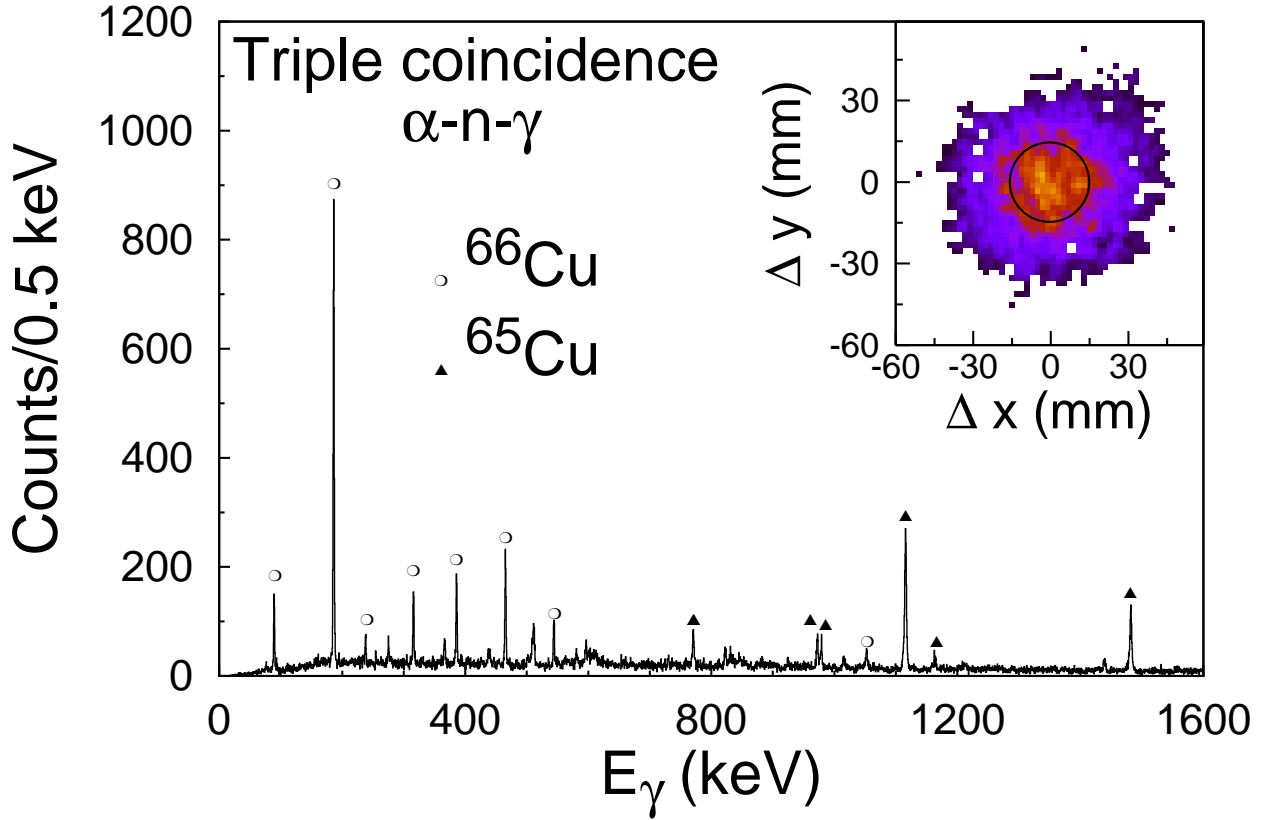


FIG. 2: (color online) Gamma spectrum in coincidence with α particles and neutrons obtained by selecting events outside the region marked in the inset (see text). The inset shows a 2D plot of the difference in positions of the detected α particle and neutron at the plane of the Si detector.

and $E_{n\alpha}$. In the 1n transfer reaction, neutrons and α particles are emitted by the breakup of ${}^5\text{He}$ in this state. Reaction kinematics restricts $\theta_{n\alpha}$ to a maximum value (θ_0) of 31° for these events. Such a directional correlation is absent in the case of 2n transfer where the neutron arises by evaporation from excited ${}^{67}\text{Cu}$ nuclei as shown in Fig. 1b. Thus the region $\theta_{n\alpha} > \theta_0$ consists of events arising from 2n transfer and the corresponding differential cross sections were obtained by restricting to events in this region. The region $\theta_{n\alpha} < \theta_0$ contains contributions from both 2n and 1n transfer. Fig. 2 shows the sum of the added-back γ -ray spectrum of the EXOGAM array in coincidence with α particles and neutrons for $\theta_{n\alpha} > \theta_0$. The prominent transitions in ${}^{66}\text{Cu}$ and those in ${}^{65}\text{Cu}$ arising from the α 2n fusion-evaporation channel are indicated. The inset shows the division of the kinematic region in a two dimensional plot of Δx vs. Δy , where Δx and Δy are the difference in positions of the detected α -particle and neutron at the plane of the Si detector. The central region (marked by a circle in the inset) represents the 31° cone. The differential cross sections for 1n transfer

were obtained by subtracting the contribution of the 2n transfer that were obtained from the yields outside the cone (scaled with the appropriate solid angles) from the total yields in this region. The emission angle of ${}^5\text{He}$ was approximated as the measured θ_α . The fraction of the solid angle of the Neutron Wall corresponding to the two regions, inside and outside the cone, were obtained from simulations.

The absolute cross sections were obtained from the known efficiencies, target thickness and integrated beam intensity. The extracted differential cross sections for 1n and 2n transfer reactions are presented in Fig. 3. Only statistical errors are shown in the figure and range from 2-3 % and 15-20 % for the 2n and 1n transfer reaction respectively. In Fig. 3, for 1n transfer, $\theta_{{}^5\text{He}}$ was assumed to be the same as θ_α . The relative insensitivity of the extracted cross sections to the precise value of θ_0 was verified by repeating the analysis with a 5° variation. The measured elastic angular distributions are shown in Fig. 3b.

Coupled Reaction Channel (CRC) calculations [2] were performed using the code FRESKO [25] to understand the angular distributions and the role of channel coupling on the various processes. The full complex remnant term and non-orthogonality correction were included. In the present calculations coupling to the breakup channel was not considered. This is based on lower breakup contribution (as compared to transfer) observed in [26] and also the reduced importance of Coulomb breakup in this lower Z target. Entrance and exit channel bare potentials consisted of double-folded real and interior Woods-Saxon imaginary parts. The M3Y effective interaction [27] and the ${}^6\text{He}$ and ${}^5\text{He}$ matter densities were from Refs. [28] and [29], respectively. The Woods-Saxon potential parameters were: $W = 50$ MeV, $R = 1.0 \times (A_p^{1/3} + A_t^{1/3})$ fm, $a = 0.3$ fm.

The positive Q-value of the ${}^{65}\text{Cu}({}^6\text{He}, {}^5\text{He}){}^{66}\text{Cu}$ reaction favors population of relatively high-lying states. However, the measured trend of $(2J+1)S$ values as a function of excitation energy derived from a direct transfer analysis in the ${}^{65}\text{Cu}(d,p)$ reaction shows a rather rapid decrease with increasing excitation energy (below ~ 3 MeV) [30]. Thus, a restricted number of states in ${}^{66}\text{Cu}$ were included as suggested from the above studies. Configurations and spectroscopic factors and neutron+ ${}^{65}\text{Cu}$ potentials were taken from [30, 31]. Transfer to the $3/2^-$ ground state resonance of ${}^5\text{He}$ was also included, with spectroscopic factor taken from Ref. [32]. The n+ ${}^5\text{He}$ binding potential was of a Woods-Saxon form with radius parameter $r_0 = 1.25$ fm, diffuseness $a = 0.65$ fm, and a spin-orbit component of the same geometry and a depth of 6 MeV.

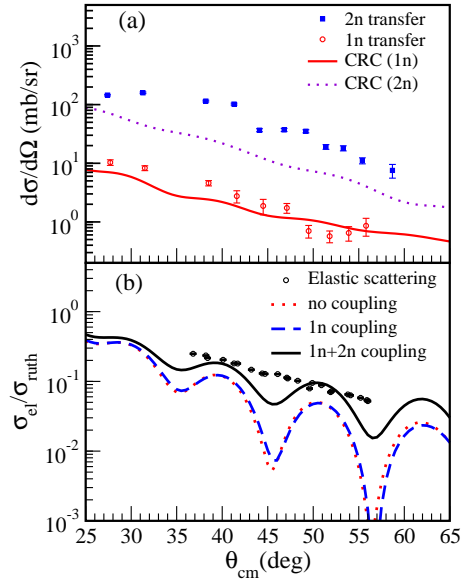


FIG. 3: (color online) Angular distributions for ${}^6\text{He} + {}^{65}\text{Cu}$ for (a) 1n and 2n transfer. CRC calculations for 1n and 2n transfer are shown. (b) Elastic scattering. CRC calculations with no coupling (dotted curve), only 1n transfer couplings (dashed line) and both 1n and 2n transfer couplings (solid line) are shown.

The inclusion of 2n transfer in the CRC calculation is more challenging, as the Q value for this reaction favors high-lying states in ${}^{67}\text{Cu}$. The Q matching conditions, together with the fact that no γ rays for transitions in ${}^{67}\text{Cu}$ were observed, suggest that if the mechanism is conventional transfer only states above the 1n separation threshold in ${}^{67}\text{Cu}$ (9.1 MeV) but below the 2n threshold (16.2 MeV) should be considered. Two-step sequential transfer was omitted, as attempting to include it would increase the number of unknown factors in the calculation. Due to the lack of detailed information on high-lying states in ${}^{67}\text{Cu}$, structural information of high lying states in ${}^{65}\text{Cu}$ observed from (p,t) studies [33] were used instead. The validity of this approximation is strengthened by the observed similarity of the low-lying spectra of ${}^{65}\text{Cu}$ and ${}^{67}\text{Cu}$. Thus, states in ${}^{67}\text{Cu}$ in the range from 10.9 to 14.3 MeV, with spins, parities and excitation energies of known states in ${}^{65}\text{Cu}$ [34] were included. A dineutron-like cluster structure for these states with the lowest possible 2n angular momentum relative to the ${}^{65}\text{Cu}$ was assumed. The $2n+{}^{65}\text{Cu}$ binding potentials were of Woods-Saxon form, radius $R = 1.25 \times (2^{1/3} + 65^{1/3})$ fm and diffuseness $a = 0.65$ fm. All spectroscopic factors were set to 1.0. The form factor for the $2n+{}^4\text{He}$ structure of

${}^6\text{He}$, was taken from Ref. [35]. The optical potential used were the same double-folded plus Woods-Saxon combination as for the other channels, with the ${}^4\text{He}$ matter density derived from the charge density of [36].

Calculated angular distributions for transfer and elastic scattering are shown in Fig. 3. The solid curve in Fig. 3a is the sum of the angular distributions for 1n transfer to the calculated individual states in ${}^{66}\text{Cu}$; the agreement with the data is good, supporting the assumption that the mechanism is conventional single neutron stripping to bound states in the target-like nucleus. The calculation for 2n transfer, denoted by the dotted line in Fig. 3a reproduces well the shape of the angular distribution. The difference in absolute magnitude is not surprising in view of the uncertainties in calculating a two neutron transfer angular distribution. The present calculations support the suggestion, prompted by the very large cross section, that the 2n transfer is largely the result of a direct, one-step transfer of a dineutron-like cluster. These calculations using the simple assumptions of a large spectroscopic factor for both configurations can be justified as the two configurations are not orthogonal to each other. This is similar to the case of ${}^6\text{Li}$ where the sum of the spectroscopic factors for the $\alpha+d$ and ${}^3\text{He}+t$ configurations is much greater than one.

The effect of the transfer couplings on elastic scattering is shown in Fig. 3b. The dotted curve shows the result of the calculation with no coupling. The dashed curve denotes the effect of coupling to 1n transfer only. It can be seen that this coupling has a small effect on the elastic scattering. The solid curve denotes the result of the calculation including both 1n and 2n transfer couplings. The effect of coupling to the 2n transfer channel can be seen to be much stronger than that due to 1n transfer, acting to further damp the oscillations and increase the larger angle cross section to better match the data. Although the elastic scattering is still oscillatory compared to the data, a problem usually associated with insufficient absorption, the magnitude of the data is well described. The fusion cross section was calculated using the in-going wave boundary condition. Calculations with no coupling, coupling to 1n transfer only and to both 1n and 2n transfer yielded values of 1655, 1631 and 1551 mb, respectively, in good agreement with the measured fusion cross section of 1396(90) mb. The influence of 1n transfer coupling on the fusion process, like that for the elastic channel is seen to be weak. The relatively good agreement between the measured and calculated values for the various channels as seen from Fig. 3 for this system represents an important step towards an understanding of the reaction mechanism for Borromean nuclei

at energies near the Coulomb barrier. De Young *et al.*[15] pointed out the large yield of α particles in reactions of ${}^6\text{He}$. In particular, the results with a ${}^{209}\text{Bi}$ target show that the ratio of 2n transfer cross section to 1n is about 2.5-3. For the medium mass target studied here, the ratio is about 10. This difference could arise from the role of target structure and different channel couplings. The present coincidence measurements show unambiguously that, there is no need to invoke transfer to states in the 2n continuum of ${}^{67}\text{Cu}$ to explain the large observed cross section.

In summary, exclusive measurements for 1n and 2n transfer, elastic scattering and fusion for the Borromean nucleus ${}^6\text{He}$ incident on a medium mass target at an energy near the Coulomb barrier are reported. The first successful application of triple coincidences, with low energy ISOL beams, between α , neutrons and γ rays from the target-like residue and their angular correlations were used to uniquely obtain the 1n and 2n transfer angular distributions. The present work shows that the main contribution to transfer arises from the 2n component, thereby indicating [10] the dominance of the di-neutron structure in ${}^6\text{He}$. CRC calculations illustrate the important role played by the coupling of the two neutron channel on the reaction mechanism. The availability of low energy beams of double Borromean ${}^8\text{He}$, having the highest N/Z ratio, would provide an excellent opportunity to study correlations between the four valence neutrons and to investigate the effect of the continuum in this drip line nucleus.

* corresponding author: navin@ganil.fr

- [1] M. Dasgupta *et al.*, Ann. Rev. Nucl. Part. Sci. 48, 401 (1998).
- [2] N. Keeley *et al.*, Prog. Part. Phys. 59, 579 (2007).
- [3] F. Barranco *et al.*, Eur. Phys. J. A 11, 385 (2001); E. Vigezzi *et al.*, Nucl. Phys. A 752, 600 (2005).
- [4] Masayuki Matsuo, Phys. Rev. C 73, 044309 (2006).
- [5] M.V. Zhukov *et al.*, Phys. Rep. 23, 1151 (1993).
- [6] T. Aumann, Eur. Phys. J. A 26, 441 (2005).
- [7] G. M. Ter-Akopian, *et al.*, Phys. Lett. B426, 251 (1998).
- [8] Yu. Ts. Oganessian *et al.*, Phys. Rev. Lett. 82, 4996 (1999).

- [9] M. Marques *et al.*, Phys. Lett. B476, 219 (2000).
- [10] L.I. Galanina *et al.*, Phys. At. Nucl. 70, 283 (2007).
- [11] P. Mueller *et al.*, Phys. Rev. Lett. 99, 252501 (2007).
- [12] N. Michel *et al.*, Phys. Rev. C 75, 031301(R) (2007).
- [13] R.K. Adair, Phys. Rev. 111, 632 (1958).
- [14] J.P. Bychowski *et al.*, Phys. Lett. B596, 26 (2004).
- [15] P.A. DeYoung *et al.*, Phys. Rev. C 71, 051601(R) (2005).
- [16] A. Navin *et al.*, Phys. Rev. C 70, 044601 (2004).
- [17] T. Matsumoto *et al.*, Phys. Rev. C 73, 051602R (2006).
- [18] M. Rodriguez-Gallardo *et al.*, Phys. Rev. C 72, 024007 (2005).
- [19] A.M. Moro *et al.*, Phys. Rev. C 75, 064607 (2007).
- [20] J. Simpson *et al.*, Heavy Ion Phys. 11, 159 (2000).
- [21] O. Skeppsted *et al.*, Nucl. Inst. Meth A 421, 531 (1999).
- [22] J. Ljungvall *et al.*, Nucl. Inst. Meth A 528, 741 (2004).
- [23] J.W. Meadows, Phys. Rev. 157, 1076 (1967).
- [24] F. Pulhofer, Nucl. Phys. A 280, 267 (1975).
- [25] I.J. Thompson, Comp. Phys. Rep. 7, 167 (1988).
- [26] J.J. Kolata *et al.*, Phys. Rev. C 75, 031302(R) (2007).
- [27] G.R. Satchler and W.G. Love, Phys. Rep. 55, 183 (1979).
- [28] J. S. Al-Khalili *et al.*, Phys. Rev. C 54, 1843 (1996).
- [29] T. Neff and H. Feldmeier, Nucl. Phys. A 738, 357 (2004).
- [30] W.W. Daehnick, Y.S. Park, Phys. Rev. 180, 1062 (1969).
- [31] M.R. Bhat, Nucl. Data Sheets 83, 789 (1998).
- [32] O.F. Nemets *et al.*, Nucleon clusters in atomic nuclei and many-nucleon transfer reactions, Ukrainian Academy of Sciences, Institute for Nuclear Research, Kiev, 1988.
- [33] J.H. Bjerregaard *et al.*, Nucl. Phys. 85, 593 (1966).
- [34] M.R. Bhat, Nucl. Data Sheets 69, 209 (1993).
- [35] L. Giot *et al.*, Phys. Rev. C 71, 064311 (2005).
- [36] J. S. McCarthy *et al.*, Phys. Rev. C 15, 1396 (1977).